Redirecting metabolic flux via combinatorial multiplex CRISPRi-mediated repression for isopentenol production in *E. coli*

Tian Tian[1,2], Jing Wei Kang[1,2,3], Aram Kang[1,2], Taek Soon Lee[1,2,*]

[1]Joint BioEnergy Institute, Emeryville, California, USA

[2]Biological Systems & Engineering Division, Lawrence Berkeley National Laboratory, Berkeley, California, USA

[3]Department of Chemical Engineering, University of California, Berkeley, California, USA

[*]Corresponding author: Dr. Taek Soon Lee, Joint BioEnergy Institute, 5885 Hollis St. 4th floor, Emeryville, CA 94608, USA; Phone: +1-510-495-2470, Fax: +1-510-495-2629, E-mail: tslee@lbl.gov

Abstract

CRISPR interference (CRISPRi) via target guide RNA (gRNA) arrays and a deactivated Cas9 (dCas9) protein has been shown to simultaneously repress expression of multiple genomic DNA loci. By knocking down endogenous genes in competing pathways, CRISPRi technology can be utilized to re-direct metabolic flux toward target metabolite. In this study, we constructed a CRISPRi-mediated multiplex repression system to silence transcription of several endogenous genes in order to increase precursor availability in a heterologous isopentenol biosynthesis pathway. To identify genomic knockdown targets in competing pathways, we first designed a single-gRNA library with 15 individual targets, where 3 gRNA cassettes targeting gene *asnA*, *prpE*, *gldA* increased isopentenol titer by 18-24%. We then combined the 3 single-gRNA cassettes into two- or three- gRNA array and observed up to 98% enhancement in production by fine-tuning the repression level through titrating dCas9 expression. Our strategy shows that multiplex combinatorial knockdown of competing genes using CRISPRi can increase production of target metabolite, while the repression level needs to be adjusted to balance the metabolic network and achieve the maximum titer improvement.

Keywords

CRISPR interference, isopentenol, metabolic flux redirection, simultaneous genome knockdown, *Escherichia coli*, Mevalonate pathway

Introduction

Optimization of metabolic flux toward targeted biosynthesis pathway is essential for high productivity and yield. To re-direct carbon flux, a common approach is to reduce the production of excessive intermediates or byproducts by deleting genes in the competing endogenous pathways[1,2]. Since cells have evolved complex regulatory metabolic network, knocking out multiple endogenous pathways is often required for the enrichment of key metabolite as precursor of the target pathway[3–7]. For example, in many cases where central metabolites such as pyruvate and acetyl-CoA were used as a precursor for heterologous biosynthesis, host cells are typically engineered by knocking out genes in organic acids production or ethanol fermentative pathways which can substantially improve titer and productivity[8–11] .

To effectively knockout or knockdown multiple endogenous competing pathway genes, consecutive and combinatorial multiplex genome editing approaches have been developed and implemented in metabolic engineering. The multiplex automated genome engineering (MAGE) method facilitates simultaneous chromosomal engineering at multiple loci[12]. However, the lack of selection of edited cells via MAGE increased the capital cost of chromosomal pathway optimization[13]. As the number of target genes in the pathway increases, a number of recursive rounds of MAGE are required to improve editing efficiency[14]. In contrast to MAGE, Cas9-mediated genome engineering using Clustered Regularly Interspaced Short Palindromic Repeats (CRISPR) system exerts strong selection toward edited cells by introducing a double strand break (DSB) in the chromosome. The successfully edited cells rely on homologous recombination at the DSB region using donor DNA with homology arms that matches the sequences flanking the DSB[15–18]. This approach tremendously improved genome editing

efficiency, while enabling scar-less genome modulation without the use of antibiotic selection[19–21].

Assisted with CRISPR technology, simultaneously editing of multiple genome loci was achieved in *Saccharomyces* species[22] and some mammalian cell lines[23]. However, for many industrial prokaryotic hosts, it is still difficult to modulate multiple places in the chromosome at the same time due to the low homologous recombination efficiency. In *E. coli*, while the editing efficiency of two genes is around 80%, the efficiency drops to 20% when targeting three genes simultaneously[24]. In some cases, the modified cells possess a phenotypic advantage; therefore screening assays can be used for enrichment of successful edits, resulting in 70% efficiency of three gene targets[25]. However, in most of the cases where no obvious phenotypic change is associated with genome editing, it is difficult to design enrichment assays to obtain high editing efficiency of multiple genes.

To bypass the low chromosomal pasting rate in many prokaryotes, CRISPR interference (CRISPRi) via a deactivated Cas9 (dCas9) protein has been utilized to repress expression of multiple genomic loci. Bound with target guide RNA (gRNA), dCas9 protein lacks catalytic activity but still retains strong specific DNA binding function, which can sufficiently suppress gene transcription[26,27]. As a multiplex genome engineering tool, CRISPRi technology has been utilized to optimize heterologous biosynthesis by knocking down both endogenous competing pathways and exogenous genes on production plasmids[28–32]. In *E. coli* terpenoid biosynthesis, for example, production of bisabolene and lycopene were enhanced by repressing plasmid-borne MVA pathway genes while production of isoprene increased by repressing endogenous gene *ispA*[33]. Similarly, in anthocyanin biosynthesis, repression of a single endogenous gene deregulated the competing methionine biosynthetic pathway and improved precursor availability

[30]. Recently, simultaneous suppression of three genes (*gabD, ybgC* and *tesB*) enhanced 1,4-butanediol biosynthesis, while repression of four genes (*pta, frdA, ldhA, and adhE*) increased n-butanol productivity and yield[32]. Not only in *E. coli*, in other industrial hosts, CRISPRi technology has also been widely studied. In *C. glutamicum*, repression for individual gene *pgi*, *pck* and *pyk* resulted in titer enhancement for L-lysine and L-glutamate production [29]. In cyanobacteria, simultaneous knockdown of 4 genes led to repression of carbon storage compounds formation during nitrogen starvation[31].

In this study, we applied CRISPRi-mediated repression of endogenous competing pathways for production of an isoprenoid-derived C5 alcohol, isopentenol. Isopentenol (or 3-methyl-3-buten-1-ol) is a biofuel blend-in and precursor for many industrial chemicals such as prenol, isoprene and isoamyl alcohol esters[34,35]. Although considerable research has been devoted to engineer the isopentenol biosynthesis pathway[36–38], little attention has been paid to vary the genetic background and re-route metabolic intermediates. To achieve sufficient isopentenol production, we employed a previous engineered, 2-plasmid biosynthesis platform by overexpressing genes encoding the MVA pathway and *nudB* to convert isopentenyl diphosphate (IPP) to isopentenol[38]. We targeted 21 individual endogenous genes in competing pathways to divert carbon flux toward IPP precursor synthesis. We then selected three of those targets with increased isopentenol titer to further perform combinatorial knockdown. We observed up to 98% enhancement in production with multiplex combinatorial repression comparing to base strain. To our knowledge, this is the first report that uses CRISPRi to systematically identify target genes in isopentenol biosynthesis. This work provides an alternative approach for genome-wide discovery of knockdown/knockout loci for metabolic engineering of the isoprenoids biosynthesis.

Results

Initial design of CRISPRi-mediated repression system for isopentenol production

To control the repression level and timing of endogenous chromosomal genes, we constructed a tetracycline-inducible dCas9 system using customized CRISPR gRNA (crRNA) array (Figure 1). The use of inducible system enabled tunable repression of genes in competing pathways which

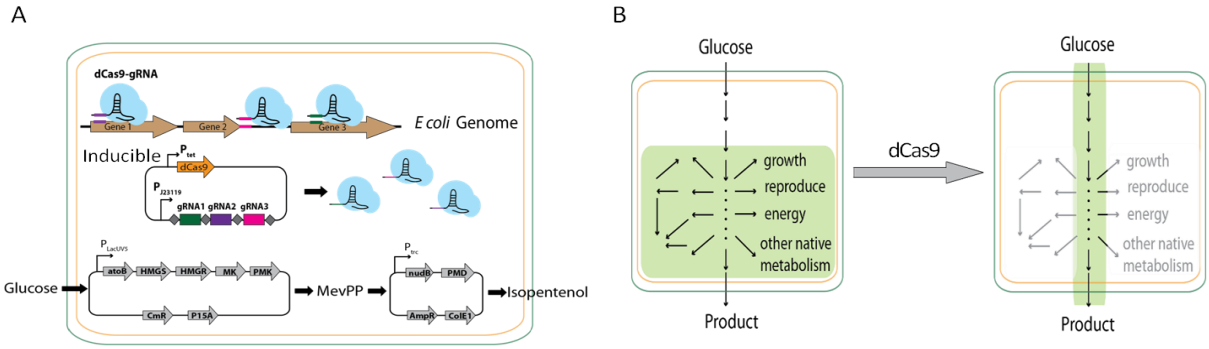

Figure 1 Schematic description of the isoprenoid production system using CRISPRi-mediated repression. (A) The isoprenoid pathway consists of two plasmids, converting glucose to 3-methyl-3-butenol. The dCas9 protein is controlled by a tetracycline-inducible promoter, and the gRNA array is controlled by a strong constitutive promoter J23100. (B) Before the induction of dCas9 protein, the cell may distribute its cellular resources and metabolic flux for growth, secondary metabolite production, energy generation and so on. After the induction of dCas9, the cell can re-direct metabolic flux toward our target production.

could include essential genes, expanding the number of chromosomal loci we can target. In addition, since permanent gene knockout and knockdown may reduce growth rate, the use of inducible CRISPRi also allowed us to control the timing of repression of chromosomal genes. Hence, before induction of CRISPRi, the metabolic flux can be distributed toward reproduction, energy generation and other metabolism necessary for rapid cell growth; after induction of dCas9, the metabolic flux can be diverted toward the target isopentenol biosynthesis pathway, which largely reduced the negative impact of gene knockdown on cell growth (Figure 1B). In addition, the CRISPR array allows multi-gene targeting with a single transcript. Compared to the design of

synthetic gRNA, CRISPR array eliminated the utility of promoter and terminator for each single gRNA, which shortened the sequence length when targeting multiple loci.

To obtain sufficient isopentenol production, we employed a previously engineered 2-plasmid isopentenol biosynthesis platform (Figure 1A). Plasmid 1 contains 5 genes expressing the heterologous MVA pathway under control of trc promoter (P_{trc}): *atoB*, *HMGS*, *HMGR*, *MK*, *PMK*, which converts central metabolite acetyl-CoA to mevalonate diphosphate; Plasmid 2 contains two genes under lacUV5 promoter (P_{lacUV5}): *nudB* and *PMD*, converting mevalonate diphosphate to isopentenol. The isopentenol production pathway will be induced after the induction of CRISPRi-mediated repression system, so that endogenous genes in the competing pathways can be fully down-regulated prior to the target pathway biosynthesis.

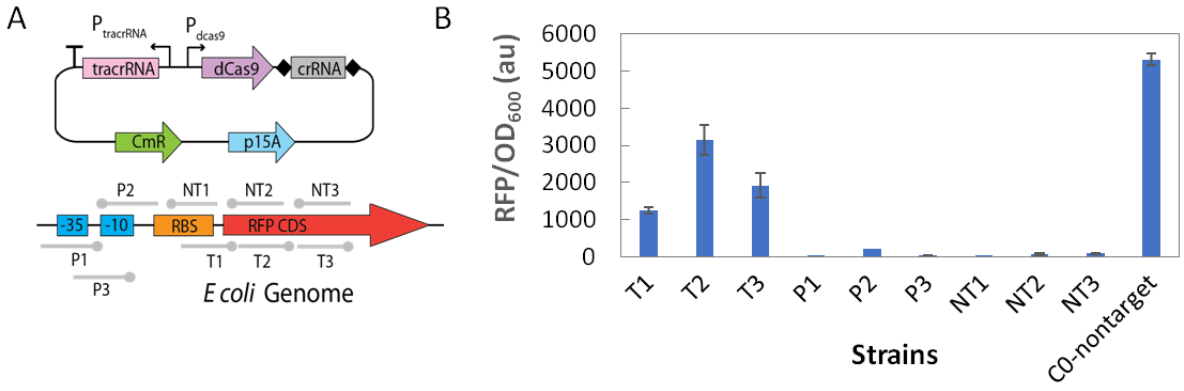

Figure 2 RFP repression efficiency with different gRNAs. (A) Top: plasmid design of the constitutively expressed dCas9 and crRNA. dCas9 was controlled by its natural promoter P_{dcas9}, crRNA was placed downstream of dCas9, also expressed from promoter P_{dcas9}. Bottom: different gRNAs targeting different DNA strands and location of RFP. P: targeting promoter region, NT: targeting non-template strand, T: targeting template strand. (B) Repression efficiency of different gRNA measured by RFP fluorescence per cell. The nontarget gRNA is a sequence that doesn't target *E. coli* genome.

To establish an initial design of CRISPRi-mediated repression system, we constructed a plasmid with dCas9 and gRNA under a natural constitutive promoter ($P_{dcas9\text{-}Marraffini}$) from *S. pyogenes*[27]. To determine the repression efficiency of a gRNA targeting different DNA strands and different locations on a gene, we used a chromosomal RFP as a reporter, and designed nine gRNA

sequences to target the RFP. This includes three gRNAs targeting promoter regions (P1, P2, P3), three gRNAs targeting non-template coding strand (NT1, NT2, NT3) and three gRNAs targeting the template coding strand (T1, T2, T3) (Figure 2). We observed higher repression efficiency targeting the non-template regions for the open reading frame. While for promoter region, targeting either strand renders similar repression level. Among all those gRNAs, we obtained 115-fold, 63-fold, and 58-fold from gRNA NT1, NT2, NT3, respectively, suggesting that targeting the beginning of transcript leads to higher repression, which is consistent to previous findings[26]. In addition, we obtained 126-fold and 128-fold repression from plasmid bearing gRNA P1 and P3, but only 24-fold repression from gRNA P2, indicating that targeting the region from -10 to -35 of promoter region has higher efficiency than targeting the region upstream of -10 of the promoter.

Optimization of a tunable CRISPRi system

In the next step, we aimed to construct a tunable CRISPR-dCas9 system to conditionally knockdown endogenous genes based on previous plasmid architecture. We selected the tetracycline-inducible promoter (P_{tet}) to drive the dCas9-gRNA repression system due to its relatively tight regulatory capability (Figure 3). We built CRISPR-dCas9 plasmid variants using NT1 gRNA sequence since it reflected high targeting efficiency (Figure 2B). And we continued to use the chromosomal RFP as a reporter to measure repression level of the CRISPRi variants. Both wild type P_{tet_wt} promoter[39] and an engineered low-leakage P_{tet_eng} promoter variant[40] were employed to drive dCas9 and gRNA expression, resulting in variant strain C1 and C2. However, neither cassette succeeded in reducing RFP gene expression upon increasing concentration of

anhydrous tetracycline (aTc). The P_{tet_wt} promoter in C1 turns out to be extremely leaky that even without adding any aTc inducer, the system repressed RFP fluorescence by 7-fold.

On the contrary, the P_{tet_eng} promoter in C2 was not leaky but failed to repress RFP expression at any inducer concentration. We suspected that this malfunction of C1 and C2 is due to the lack of gRNA level, as insufficient gRNA expression can cause complex non-linear repression behavior or no repression at all[24,33]. Therefore, we inserted a strong constitutive promoter P_{J23119} upstream of the gRNA sequence, generating C3 and C4 from C1 and C2. Consequently, the leakiness of C3 system has been substantially reduced. Also, C4 system efficiently decreased RFP fluorescence at varying inducer concentrations while maintained its tight regulation.

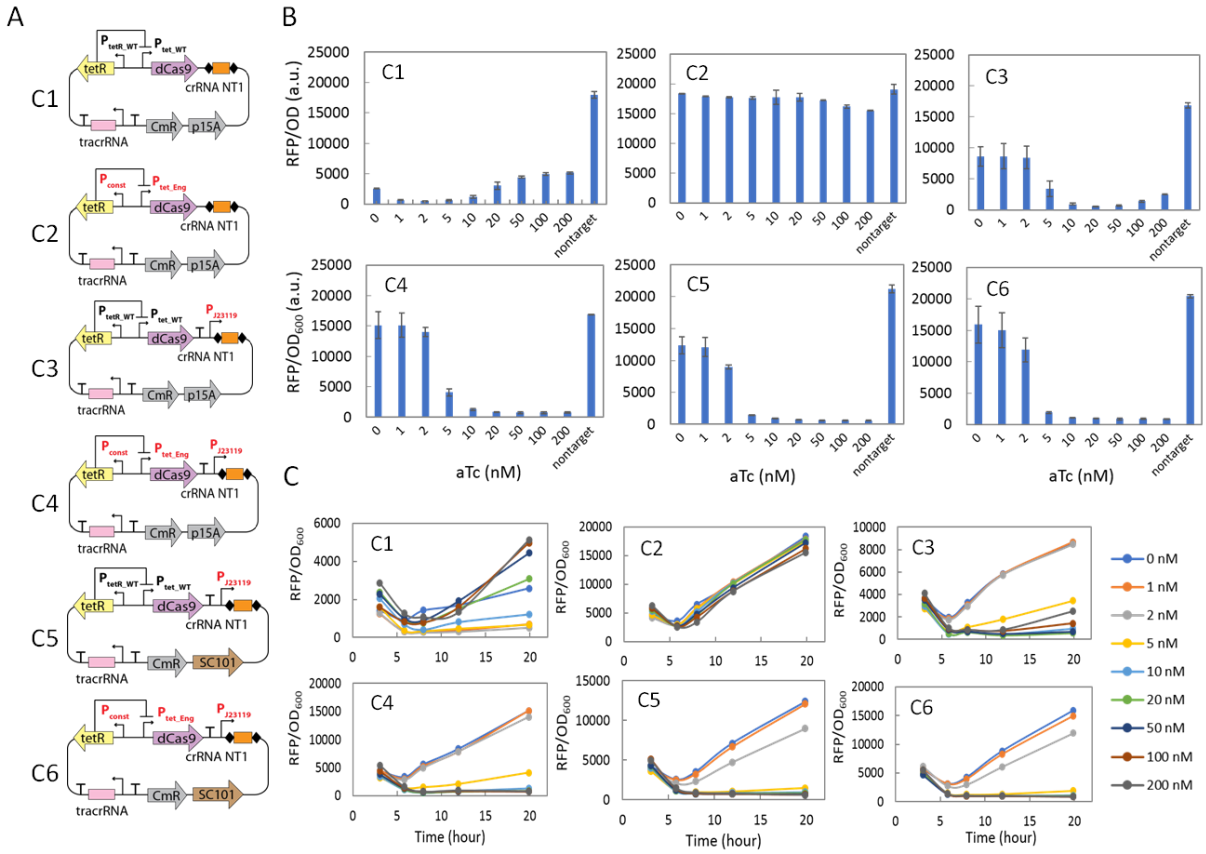

Figure 3 Construction and characterization of CRISPR-dCas9 repression cassettes. (A) Schematics of CRISPR-dCas9 variants with different promoters driven *dCas9*, *crRNA* and *tetR* gene. Red color is used in promoter names to emphasize the difference in each system. (B) Characterization of repression efficiency of different cassettes with varying anhydrous tetracycline inducer concentrations. (C) Time-course repression response of different cassettes with varying inducer concentrations.

To reduce the metabolic burden of overexpressing dCas9 protein[41], we replaced the replication origin of plasmids in C3 and C4 from a medium copy (p15A) to a low copy origin (SC101). The resultant strains C5 and C6 both remains their high repression efficiency, while C5 is still leakier than C6. Without adding any inducer, the RFP fluorescence for C5 and C6 is 42% and 22% less than the control strain harboring non-targeting gRNA respectively (Figure 3B).

To investigate the expression kinetics for genes targeted by CRISPR-dCas9 system, we measured the RFP fluorescence change over time among different plasmid variants. Except for C1 and C2, the RFP fluorescence in other strains can be reduced to >50% after 6 hours, >85% after 9 hours, and >90% after 20 hours of its wild type with 5 nM aTc (Figure 3C). Considering RFP is engineered with high protein stability and long half-life, we anticipated that when applying this repression system to regulate endogenous *E. coli* genes, their protein level may decrease faster than our current RFP data due to higher degradation rate. Based on this analysis, we chose to induce expression of the isopentenol pathway 6 hours after activating the CRISPRi-mediated repression system.

CRISPRi negatively affects gene expression in the same operon

Since dCas9 protein represses gene expression at a transcription level, we explored whether targeting one gene using CRISPR-gRNA in an operon will affect the expression level of the rest of genes. We constructed a bicistronic operon on plasmid with RFP as an upstream and GFP as a downstream gene. Both genes are regulated by a constitutive synthetic promoter P_{J23100} (Figure 4).

We designed three gRNAs targeting the promoter (P), the beginning of RFP coding sequence (RFPNT) and the beginning of GFP coding sequence (GFPNT). We used plasmids (JBEI-18655,

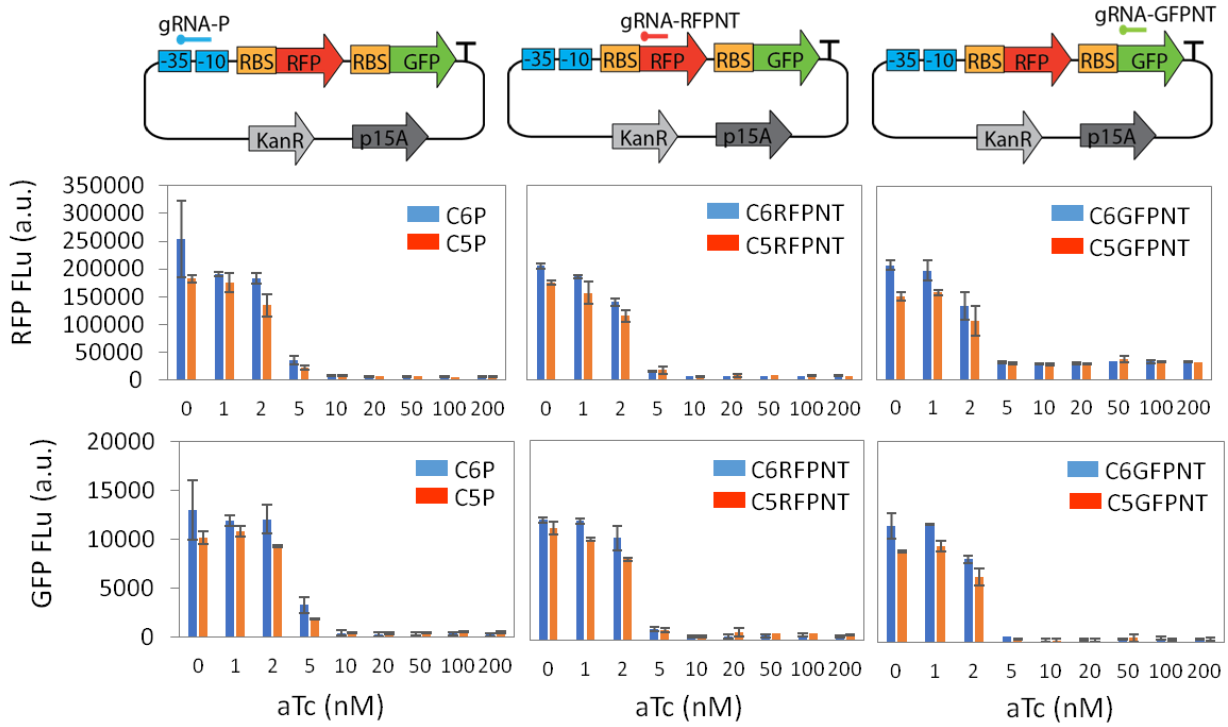

Figure 4 Repression properties of CRISPR-dCas9 system for genes in an operon. Top: Schematics indicating the location of target gRNA in the operon. Middle: RFP fluorescence in response to different gRNA. Bottom: GFP fluorescence in response to different gRNA.

JBEI-18648) from strain C5 and C6 to construct the repression systems bearing those gRNAs and transformed both the repression plasmids and the RFP-GFP operon plasmid (JBEI-18698) into the cells, creating strains C5P, C5RFPNT, C5GFPNT, C6P, C6RFPNT, C6GFPNT. Since dCas9 inhibits transcription of mRNA, we hypothesized that by targeting the upstream transcript, the downstream transcript will no longer be expressed. As we expected, for both C5- and C6-based systems, targeting the promoter region and RFP coding sequence led to over 95% reduction in both RFP and GFP fluorescence while targeting GFP coding sequence led to over 97% decrease in GFP fluorescence with respect to the wild type controls. However, to our surprise, we observed 79% and 86% RFP fluorescence reduction respectively in C5GFPNT and

C6GFPNT by only targeting the downstream GFP coding sequence. We postulated that targeting the downstream mRNA will shorten the entire transcript and may also decrease the mRNA stability, which may result in reduced expression. However, to draw any conclusion, RNA level should be quantified for both RFP and GFP with the three gRNAs, which could be an interesting scope to explore in the future.

When varying the inducer concentration for our CRISPRi system, we observed a sharp decrease (up to 28-fold) in the targeted gene expression between 0 and 5 nM aTc; then, a relatively low repression (up to 8-fold) between 5 nM and 10 nM aTc; and limited change in signal (up to 1.5-fold) with higher inducer concentration (Figure 2 and 3). This observation indicates that our system exhibits a step-change behavior. Therefore, we next chose 0, 5 and 10 nM inducer concentration to control the repression strength in the genome-wide knockdown experiments.

Efficient multiplex repression of CRISPRi system reduced acetate production

To test whether our repression system can efficiently down-regulate multiple endogenous genes simultaneously, we constructed CRISPR array carrying multiple gRNAs using both C5- and C6-based cassette architectures (Figure 5B). The gRNA array is composed of spacer-repeat blocks that are processed into mature targeting gRNAs by the wildly conserved endogenous RNase III[42]. In *E. coli*, enzymes encoded by *poxB* converts pyruvate to acetate and genes *pta* and *ackA* encode enzymes converting acetyl-CoA to acetate (Figure 5A). Previous studies have reported that the deletion of only *poxB* or the deletion of only *ackA-pta* operon does not reduce the acetate production in wild type *E. coli* cells[8]. Taking advantage of this knowledge, we hypothesized that if our repression cassette functions efficiently for multi-gene repression, our crRNA array carrying three gRNAs targeting *poxB*, *ackA* and *pta* genes can reduce acetate formation, while a

strain harboring single-gRNA dCas9 plasmid will still produce acetate to the level comparable to that of wild type cells.

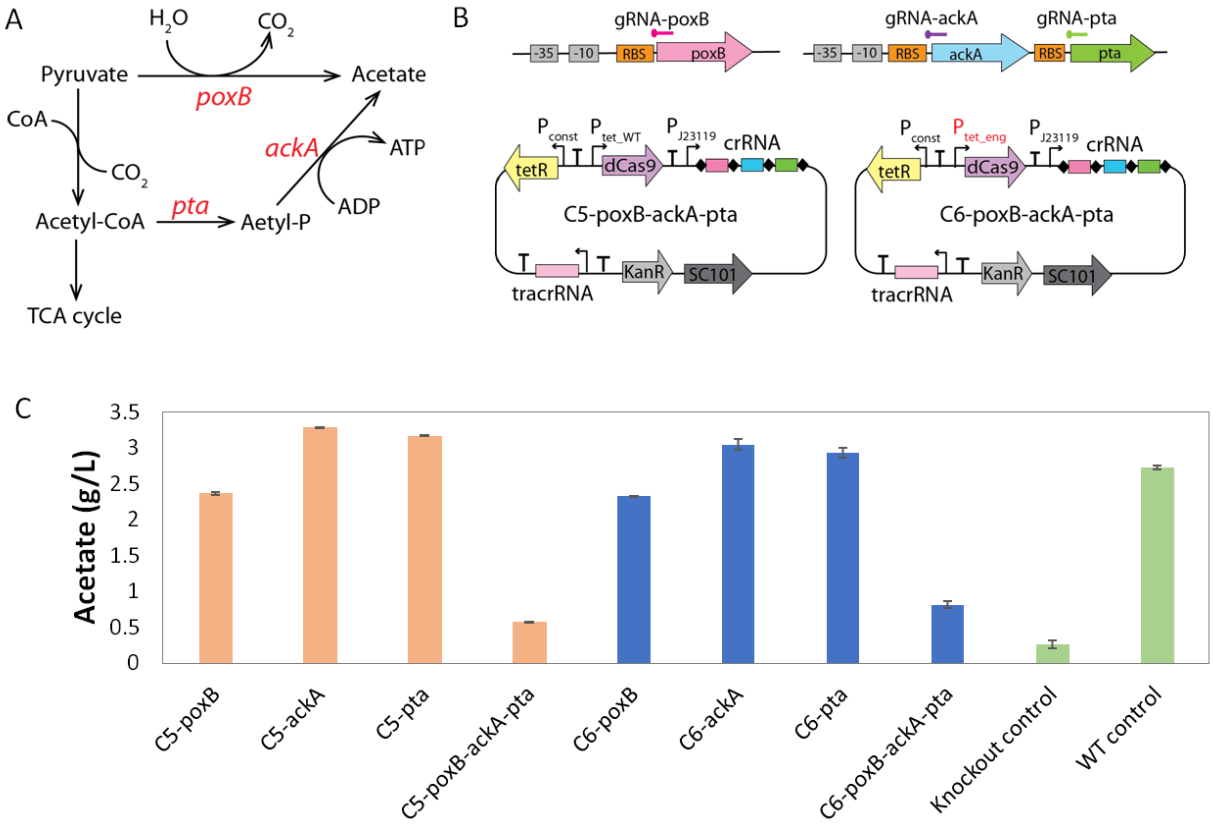

Figure 5 Implementation of multi-gRNA CRISPR-dCas9 system for inhibition of acetic acid formation. (A) schematic description of the acetate production pathway in *E. coli*. (B) Schematic description of repression cassettes based on pC5 and pC6 plasmids bearing three-gRNA array targeting gene *poxB*, *ackA*, *pta* in the chromosome. (C) Acetate formation between wild type *E. coli*, knockout strain and strains bearing different gRNA arrays.

We used a strain with *pta*, *poxB* and *ackA* knockouts as a positive control, and *E. coli* wild type strain as a negative control, both strains harbored an empty plasmid vector. After growing strains for overnight, we inoculated the cells in EZ rich medium with 1% glucose, while inducing the dCas9 protein with 10 nM aTc. After 24 hours, cells were harvested, and the acetate levels were measured by HPLC. As expected, the acetate level with triple-gRNA repression plasmid decreased by 4.8-fold for strain C5-poxB-ackA-pta and 3.4-fold for strain C6-poxB-ackA-pta

(Figure 5C). In contrast, slightly elevated acetate levels were observed with strains harboring single-gRNA targeting *pta* or *ackA* gene (C5-ackA, C5-pta, C6-ackA, C6-pta), which is consistent with the findings by Goh et al, indicating that acetate may be produced via an alternative pathway[11]. Comparing to the knockout strain, strain C5-poxB-ackA-pta still generated 2.2-fold more acetate, which may be resulted by the delay in repression due to induction kinetics or the incomplete repression of knockdown system. These data demonstrated that our CRISPRi system can efficiently down-regulate multiple endogenous genes at the same time. Since the strain C5-poxB-ackA-pta produced less acetate than the C6-poxB-ackA-pta strain, in the next step, we selected C5-based system to perform knockdown experiment to re-directing metabolic flux for isopentenol production.

Redirecting metabolic flux for isopentenol production

To identify repression targets in competing pathways for isopentenol production, we selected 15 genes based on previously selected knockout targets for lycopene or carotenoid production using MEP pathway. Since both MEP and MVA pathway shares the same precursor IPP, we hypothesize that the knockout gene targets identified for MEP pathway to improve IPP and DMAPP accumulation may also apply for isopentenol production using MVA pathway. We also selected 3 additional genes *gltA*, *accA* and *ispA*, which catalyze the key steps in TCA cycle, fatty acids synthesis, and FPP production using IPP as precursor metabolite, respectively (Figure 6A). All together, we constructed 18 single-gRNA based on C5 version of plasmid and co-transformed them with the $KG1_{R10}$ isopentenol production strain[38]. Meanwhile, plasmid from C5-poxB-ackA-pta was also co-transformed into strain $KG1_{R10}$ expecting isopentenol titer

improvement in this strain by decreasing flux to acetate. We also introduced an empty vector plasmid into cells harboring production plasmids as control (base strain).

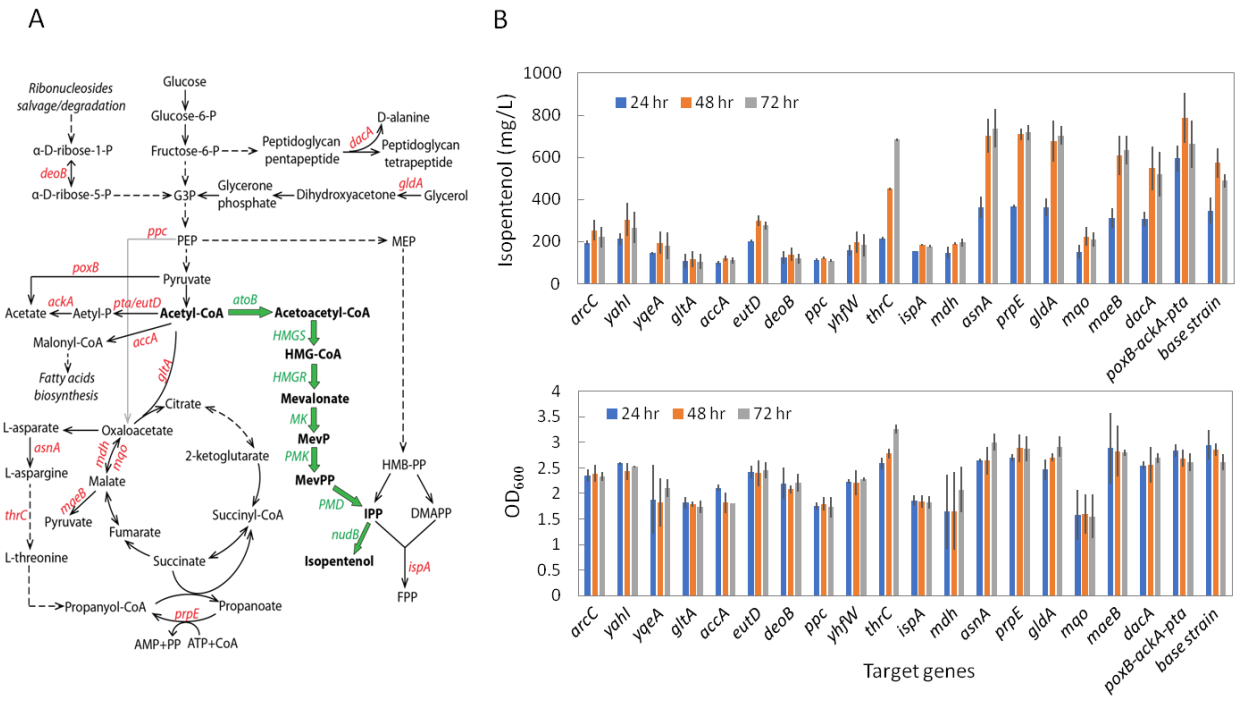

Figure 6 Re-directing metabolic flux toward isopentenol production using CRISPR-dCas9 repression system. (A) Pathway map of gene knockdown target. Red colored genes are the knockdown targets, green colored genes are overexpressed on two plasmids. (B) Isopentenol production (top) and growth (bottom) with dCas9-gRNA plasmids targeting different genes.

Upon inoculation, CRISPRi was activated with 10 nM aTc, and after 6 hours, the production pathway was induced by adding IPTG for isopentenol biosynthesis. Samples were taken for isopentenol production measurement at 24, 48 and 72 hours. We found that strain harboring the triple-gRNA plasmid targeting the acetate formation pathway improved isopentenol production by 37%. Strains C5-asnA, C5-gldA, C5-prpE bearing single-gRNA also improved isopentenol production by 18-24%, where genes *asnA*, *gldA*, *prpE* are involved in asparagine production, glycerol utilization, and propionyl-CoA synthesis, respectively (Figure 6B). We observed strong

correlation between biomass accumulation and isopentenol production (R^2=0.78), which indicated that down-regulation of some genes slowed down the cell growth, thus reduced the final titer of production.

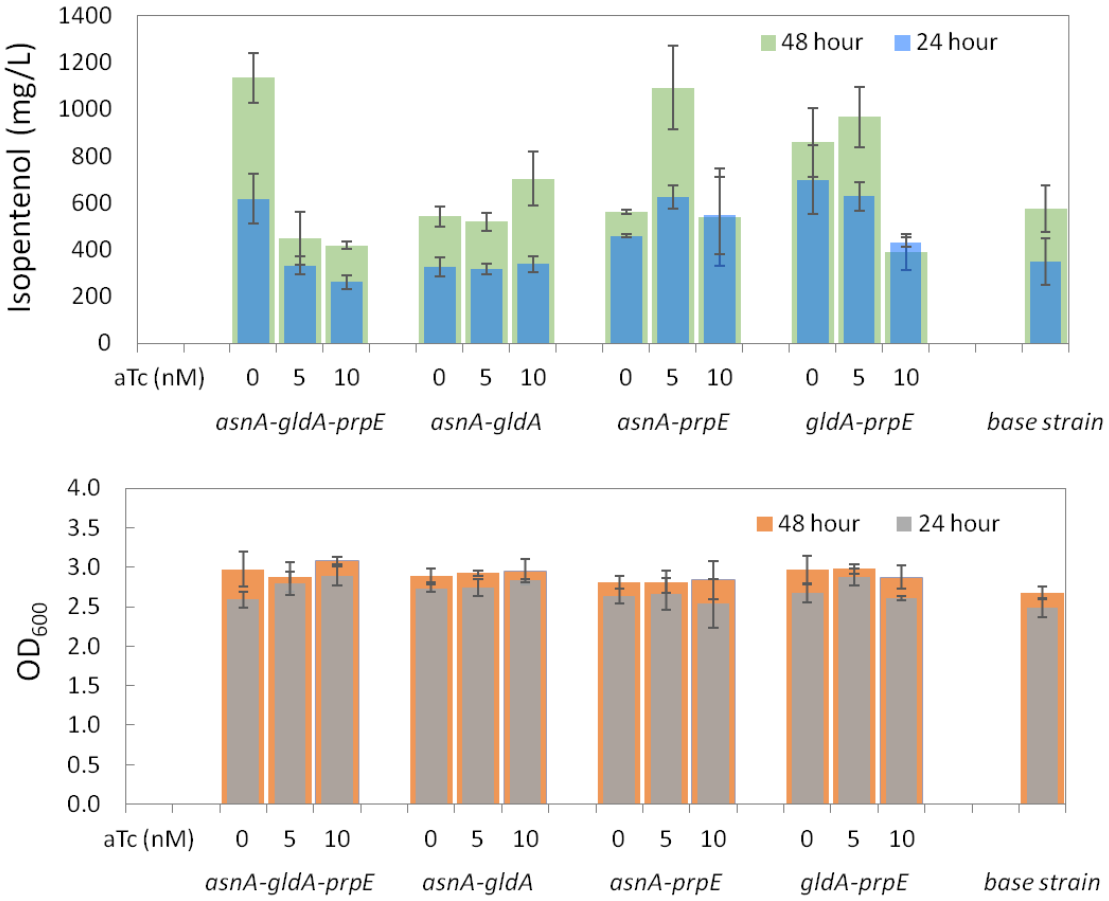

Figure 7 Combinatorial multiplex repression using CRISPR-dCas9 system for isopentenol production. Isopentenol production (top) and cell density data (bottom) after 24 and 48 hours. On the x-axis, top row shows anhydrous tetracycline concentration, bottom row shows the targeted multiple genes using CRISPR-dCas9 system.

In the next step, we combined the three gRNAs targeting *asnA*, *gldA*, *prpE* into two- and three-gRNA arrays and co-transformed them into $KG1_{R10}$, creating strain C5-asnA-gldA, C5-asnA-prpE, C5-gldA-prpE, and C5-asnA-gldA-prpE (Figure 7). We varied the magnitude of repression

by adding inducer at 0, 5, 10 nM. As previously shown, the uninduced CRISPRi system is responsible for 42% RFP fluorescence reduction with respect to its wild type control, due to the leaky expression of P_{tet_wt} (Figure 3B). We speculated that repression of endogenous genes could occur at lower rate in the absence of aTc. We observed 98% improvement in isopentenol production from C5-asnA-gldA-prpE at 0 nM aTc compared to the base strain, suggesting that relatively weak simultaneous repression of three genes *asnA*, *gldA* and *prpE*, can result in considerable improvement in isopentenol production. For the two-gRNA arrays, we observed 90% and 69% improvement, respectively in strain C5-asnA-prpE and C5-gldA-prpE with 5 nM aTc, which indicates that a relatively high level of repression is required when the combination of two genes *asnA, prpE* or *gldA, prpE* are targeted. These results imply that while individual gene knockdown may have low impact in diverting metabolic flux, selective combinatorial multiplex repression of those genes could lead to substantial improvement in production. In addition, since the improvement of isopentenol production was obtained with different repression levels, we concluded that knockdown of genes in competing pathways may need to be tuned to balance the metabolic flux, so that the repressed genes can still be expressed to some extent for maintaining normal cellular function, while resources can be re-directed toward target metabolite to increase precursor accumulation.

Discussion

In this work, we investigated the impact of CRISPRi on gene expression in polycistronic operon. We observed that by targeting the middle of an mRNA, not only the downstream transcription can be dramatically inhibited; the upstream gene expression can also be reduced to some extent possibly due to mRNA stability decrease (Figure 4). In *E. coli*, an estimation of 40.53% of genes

present in pairs and clusters[43]. Fortunately, most of the clustered genes are functionally related; therefore, when targeting one gene in an operon using CRISPRi system, it may lead to a coordinated effect by repressing other functionally-related genes in the same operon[44,45]. However, in the cases where polycistronic genes exhibit functional dissimilarities, the use of CRISPRi to repress genes in operons needs to be reevaluated and reconsidered.

In constructing the inducible CRISPRi system, we found that the uninduced condition accounts for 42% RFP fluorescence reduction of its wild type control due to the leaky expression of P_{tet_wt} promoter. Later in our production experiment, this uninduced P_{tet_wt} also result in 98% improvement in isopentenol titer. These observations imply that CRISPR system can efficiently target genomic DNA with even a residual promoter activity, which is consistent with previous research by Garst and co-workers[46]. In their study, the uninduced Cas9 was reported to achieve 80% genome editing due to leaky pBAD expression, while the induced Cas9 achieved 90% efficiency[46]. Additionally, considering RFP is optimized with enhanced stability, its half-life is about 26 hours[47], while most of *E. coli* native proteins have half-lives about 2 to a few hours[48], the reduction in protein expression of *E. coli* native genes by uninduced CRISPRi during isopentenol production experiment may be greater than 42%.

The use of inducible promoter to control the expression of dCas9 protein enables tunable knockdown of target genes. By changing the inducer concentration, we substantially improved isopentenol production at varying levels of repression when targeting different combinations of genes. These results suggest that the repression strength needs to be adjusted to balance the flux toward making desired product and maintaining normal cellular functions. Hence, a tunable knockdown system can be a powerful tool in identifying the “sweet spot” in re-directing metabolic flux for production optimization. Our finding is also in agreement with previous study

using synthetic small RNA (sRNA) to construct fine-tuned knockdown system, where the authors discovered that relatively low expression of sRNAs is needed for putrescine overproduction and relatively high expression of sRNAs is needed for L-proline production[49].

As an emerging tool for modulating endogenous gene expression, CRISPRi has been used in various biosynthesis pathways in *E. coli* including production of anthocyanin, n-butanol, 1,4-butanediol, isoprene, lycopene and bisabolene[28,30,32]. All without exception, the selected knock-down genes using CRISPRi system in those biosynthesis pathways have been previously known deletion targets. In contrast, we identified novel knock-down gene targets, which could potentially be used for a variety of monoterpenes and sesquiterpene biosynthesis since the terpenoid pathways share universal building block (IPP). We found three genes *asnA*, *gldA*, and *prpE* responsible for L-aspargine formation, glycerol utilization and propanyol-CoA synthesis, respectively, can lead to higher isopentenol production. While targeting those individual genes only generated moderate titer improvement, a simultaneous down-regulation of these three genes rendered almost 2-fold increase in production. As a result, we provided another example that CRISPRi can be a potential high-throughput screening tool to determine endogenous targets. Those identified targets can be further tested for chromosomal knockout or knockdown to generate a more stable genomic background.

Conclusion

In the present work, we developed a combinatorial multiplex repression system using CRISPRi to conditionally down-regulate endogenous genes in competing pathways for isopentenol production. We designed plasmid harboring dCas9 and gRNA array with SC101 replication origin and gentamicin resistance, which is easily compatible with commonly used production

vectors for a variety of chemical biosynthesis. By targeting three genes *poxB*, *ackA* and *pta* in acetate production pathway, we obtained 4.8-fold decrease in acetate with respect to control strain, which demonstrated that our CRISPRi system can effectively repress multiple genes simultaneously. Additionally, we employed CRISPRi to divert metabolic flux toward isopentenol production by repressing genes in competing pathways. We first created a single-gRNA CRISPRi library targeting 15 individual chromosomal loci in competing pathways. We then selected the single-gRNA with improved isopentenol production and constructed double and triple gRNA array in combination. The resultant gRNA arrays generated up to 98% increase in isopentenol titer, which suggested that CRISPRi can be used as an alternative approach to identify novel knockdown targets for balancing metabolic pathways.

Materials and Methods

Construction of plasmids

To construct constitutively expressed dCas9 cassette targeting different DNA strands and locations of RFP reporter gene in the chromosome (strain JBEI-14034), golden gate assembly method was employed and the plasmid pdCas9-Marraffini was used as base plasmid[27]. pdCas9-Marraffini used a constitutive promoter to control dCas9 protein and crRNA, with ColE1 origin and CmR marker on the vector. The resultant 9 plasmids (JBEI-18664, JBEI-18662, JBEI-18661, JBEI-18658, JBEI-18657, JBEI-18665, JBEI-18679, JBEI-18676, JBEI-18674), targeting different DNA strands and locations were transformed into strain JBEI-14034 to test their repression efficiencies.

To construct tetracycline inducible dCas9 system, Gibson assembly was employed using JBEI-18679 as base plasmid, which targets the beginning of non-template region of RFP. 6 different

cassettes were constructed (JBEI-18647, JBEI-18652, JBEI-18653, JBEI-18654, JBEI-18655, JBEI-18648), whose repression efficiency was tested by measuring RFP fluorescence reduction. Two P_{tet} promoters were tested, P_{tet_wt} is the wild type promoter from JBEI parts registry[39], P_{tet_eng} is the engineered promoter from iGem parts registry[50]. JBEI-18647, JBEI-18653, JBEI-18655 contains wild type P_{tet} promoter and the rest contains engineered Tet promoter. For each tetracycline-inducible dCas9 system, we also built its corresponding non-targeting plasmid (JBEI-18670, JBEI-18669, JBEI-18667, JBEI-18692, JBEI-18689, JBEI-18697).

To construct plasmids targeting RFP and GFP genes in the same operon, JBEI-18655 was used to generate JBEI-18650, JBEI-18651 and JBEI-18649 targeting the promoter of RFP, the RFP coding sequence and the GFP coding sequence respectively. While JBEI-18648 was used to generate JBEI-18671, JBEI-18672 and JBEI-18673 targeting the promoter of RFP, the RFP coding sequence and the GFP coding sequence respectively. JBEI-18655 and JBEI-18648 were also used to generate plasmids to target *poxB*, *ackA* and *pta* genes. For isopentenol production, only JBEI-18655 was used to generate plasmids to target the 18 newly identified genes individually and in combination.

Strains, medium and growth

For fluorescence test, *E. coli* DH1 strain harboring two plasmids, pJ23100-RFP-GFP and the corresponding dCas9-gRNA plasmid were cultured in LB. Cell cultures were first cultured in tubes overnight then diluted to fresh LB with anhydrous tetracycline in 96-well deep-well plate to OD about 0.02. The Tecan plate reader automatically read OD and fluorescence in every 20 minutes for 20 hours.

For production test, *E. coli* DH1 was co-transformed with two isopentenol production plasmids and a repression plasmid with dCas9 gene and gRNA targeting chromosomal genes. Culture was

first grown in LB for overnight, and then transferred into 5 mL EZ rich medium with 1% glucose and 10 nM anhydrous tetracycline (aTc) in culture tube at 37°C. After 6 hours, when OD of cells reached 1,500 μM isopropyl β-D-1-thiogalactopyranoside (IPTG) was added to induce the cells, and then cells were grown at 30°C. At 24, 48, and 76-hour post-induction, 250 μL culture were sampled and diluted into 250 μL of ethyl acetate spiked with n-butanol as an internal standard.

Analysis and detection of isopentenol

For isopentenol quantification, 250 μL of cell culture was combined with 250 μL of ethyl acetate containing 1-butanol (32 mg/L) as an internal standard. This mixture of ethyl acetate and cell culture was vigorously shaken for 15 min and subsequently centrifuged at 15,000g for 2 min to separate ethyl acetate from the aqueous phase. 100 μL of the ethyl acetate layer was diluted 5-fold, and 1 μL was analyzed by Agilent GCMS equipped with Cyclosil-B column (Agilent, USA) or Thermo GCFID equipped with DB-WAX column (Agilent, USA) for quantitation of isopentenol.

The method used by the GCMS has the following settings: inlet at 250°C, 1 mL/min constant flow, sample 1 μL from each vial. The oven was started at 45°C for 2 min, first ramped to 150°C at 12°C/min, then ramped to 250°C at 40°C/min, and held at 250°C for 1 min. The method used by GCFID has the following settings: The oven was started at 40°C, first ramped to 100°C at 15°C/min, then ramped to 230°C at 40°C/min, and held at 230°C for 3 min.

Analysis and detection of RFP and GFP fluorescence

For measurements taken by plate reader, RFP fluorescence was measured on an Infinite F200 PRO (Tecan, Männedorf, Switzerland) for 20 hours, with excitation at 575±10 nm and emission at 620±10 nm. All fluorescence values were normalized to cell density by measuring optical density at 600 nm (OD_{600}). For measurements using flow cytometer, 10 μL samples were added

to 200 μL Phosphate Buffered Saline (PBS) supplemented with 2 mg/mL kanamycin for halting growth. Single-cell RFP and GFP fluorescence from at least 50,000 cells were recorded by a BD C6 Accuri flow cytometer (BD Bioscience, USA). GFP fluorescence was measured with FL1 detector and RFP fluorescence was measured with FL4 detector. The average expression level was determined by taking the average of the fluorescence distribution and subtracting the average auto-fluorescence of wild type *E. coli* strain.

Author Information

Corresponding Author

Dr. Taek Soon Lee, Joint BioEnergy Institute, 5885 Hollis St. 4th floor, Emeryville, CA 94608, USA; Phone: +1-510-495-2470, Fax: +1-510-495-2629, E-mail: tslee@lbl.gov

Author Contribution

TT and TSL conceived the project, drafted the manuscript, reviewed and edited the final manuscript. TT, JWK, and AK performed the experiments and analyzed data.

Acknowledgments

We thank Drs. Daisuke Koma and Connie Kang for providing JBEI-14034 and JBEI-3606 strains, respectively. This work was part of the DOE Joint BioEnergy Institute (http://www.jbei.org) supported by the US Department of Energy, Office of Science, Office of Biological and Environmental Research, through contract DE-AC02-05CH11231 between Lawrence Berkeley National Laboratory and the US Department of Energy. This work was supported by Cooperative Research and Development Agreement (CRADA) No. FP00003594

between the Regents of the University of California /Lawrence Berkeley National Laboratory and Technology Holding LLC.

Financial Interest

Taek Soon Lee has a financial interest in Maple Bio.

Reference

(1) Li, Y., and Wang, G. (2016) Strategies of isoprenoids production in engineered bacteria. *J. Appl. Microbiol. 121*, 932–940.

(2) Kang, A., and Lee, T. S. (2015) Converting Sugars to Biofuels: Ethanol and Beyond. *Bioengineering 2*, 184–203.

(3) Jin, Y. S., and Stephanopoulos, G. (2007) Multi-dimensional gene target search for improving lycopene biosynthesis in Escherichia coli. *Metab. Eng. 9*, 337–347.

(4) Shen, C. R., and Liao, J. C. (2008) Metabolic engineering of Escherichia coli for 1-butanol and 1-propanol production via the keto-acid pathways. *Metab. Eng. 10*, 312–320.

(5) Matsuda, F., Ishii, J., Kondo, T., Ida, K., Tezuka, H., and Kondo, A. (2013) Increased isobutanol production in Saccharomyces cerevisiae by eliminating competing pathways and resolving cofactor imbalance. *Microb. Cell Fact. 12*, 1–11.

(6) Alper, H., Miyaoku, K., and Stephanopoulos, G. (2005) Construction of lycopene-overproducing E . coli strains by combining systematic and combinatorial gene knockout targets *23*, 612–616.

(7) Yu, A. Q., Pratomo Juwono, N. K., Foo, J. L., Leong, S. S. J., and Chang, M. W. (2016) Metabolic engineering of Saccharomyces cerevisiae for the overproduction of short branched-

chain fatty acids. *Metab. Eng. 34*, 36–43.

(8) Dittrich, C. R., Vadali, R. V., Bennett, G. N., and San, K. Y. (2005) Redistribution of metabolic fluxes in the central aerobic metabolic pathway of E. coli mutant strains with deletion of the ackA-pta and poxB pathways for the synthesis of isoamyl acetate. *Biotechnol. Prog. 21*, 627–631.

(9) Causey, T. B., Shanmugam, K. T., Yomano, L. P., and Ingram, L. O. (2004) Engineering Escherichia coli for efficient conversion of glucose to pyruvate. *Proc. Natl. Acad. Sci. U. S. A. 101*, 2235–40.

(10) Hu, Z. (2010) Methods and compositions for producing fatty alcohols 1–182.

(11) Goh, E. B., Baidoo, E. E. K., Burd, H., Lee, T. S., Keasling, J. D., and Beller, H. R. (2014) Substantial improvements in methyl ketone production in E. coli and insights on the pathway from in vitro studies. *Metab. Eng. 26*, 67–76.

(12) Wang, H. H., Isaacs, F. J., Carr, P. A., Sun, Z. Z., Xu, G., Forest, C. R., and Church, G. M. (2009) Programming cells by multiplex genome engineering and accelerated evolution. *Nature 460*, 894–8.

(13) Ng, C. Y., Farasat, I., Maranas, C. D., and Salis, H. M. (2015) Rational design of a synthetic Entner-Doudoroff pathway for improved and controllable NADPH regeneration. *Metab. Eng. 29*, 86–96.

(14) Wang, H. H., and Church, G. M. (2011) Multiplexed genome engineering and genotyping methods: Applications for synthetic biology and metabolic engineering. *Methods Enzymol.* 1st ed. Elsevier Inc.

(15) Jiang, W., Bikard, D., Cox, D., Zhang, F., and Marraffini, L. a. (2013) RNA-guided editing of bacterial genomes using CRISPR-Cas systems. *Nat Biotechnol 31*, 233–239.

(16) Hsu, P. D., Lander, E. S., and Zhang, F. (2014) Review Development and Applications of CRISPR-Cas9 for Genome Engineering. *Cell 157*, 1262–1278.

(17) Chari, R., Mali, P., Moosburner, M., and Church, G. M. (2015) Unraveling CRISPR-Cas9 genome engineering parameters via a library-on-library approach. *Nat. Methods 12*, 823–826.

(18) Sternberg, S. H., Redding, S., Jinek, M., Greene, E. C., and Doudna, J. A. (2014) DNA interrogation by the CRISPR RNA-guided endonuclease Cas9. *Nature 507*, 62–67.

(19) Liao, J. C., Mi, L., Pontrelli, S., and Luo, S. (2016) Fuelling the future: microbial engineering for the production of sustainable biofuels. *Nat. Rev. Microbiol. 14*, 288–304.

(20) Wang, Z., and Cirino, P. C. (2016) New and improved tools and methods for enhanced biosynthesis of natural products in microorganisms. *Curr. Opin. Biotechnol. 42*, 159–168.

(21) Fineran, P. C., and Dy, R. L. (2014) Gene regulation by engineered CRISPR-Cas systems. *Curr. Opin. Microbiol. 18*, 83–89.

(22) Jakočinas, T., Bonde, I., Herrgård, M., Harrison, S. J., Kristensen, M., Pedersen, L. E., Jensen, M. K., and Keasling, J. D. (2015) Multiplex metabolic pathway engineering using CRISPR/Cas9 in Saccharomyces cerevisiae. *Metab. Eng. 28*, 213–222.

(23) Zetsche, B., Heidenreich, M., Mohanraju, P., Fedorova, I., Kneppers, J., Degennaro, E. M., Winblad, N., Choudhury, S. R., Abudayyeh, O. O., Gootenberg, J. S., Wu, W. Y., Scott, D. A., Severinov, K., Van Der Oost, J., and Zhang, F. (2017) Multiplex gene editing by CRISPR-Cpf1 using a single crRNA array. *Nat. Biotechnol. 35*, 31–34.

(24) Li, Y., Lin, Z., Huang, C., Zhang, Y., Wang, Z., Tang, Y., Chen, T., and Zhao, X. (2015) Metabolic engineering of Escherichia coli using CRISPR-Cas9 meditated genome editing. *Metab. Eng. 31*, 1–9.

(25) Zhu, X., Zhao, D., Qiu, H., Fan, F., Man, S., Bi, C., and Zhang, X. (2017) The

CRISPR/Cas9-facilitated multiplex pathway optimization (CFPO) technique and its application to improve the Escherichia coli xylose utilization pathway. *Metab. Eng. 43*, 37–45.

(26) Qi, L. S., Larson, M. H., Gilbert, L. A., Doudna, J. A., Weissman, J. S., Arkin, A. P., and Lim, W. A. (2013) Repurposing CRISPR as an RNA-γuided platform for sequence-specific control of gene expression. *Cell 152*, 1173–1183.

(27) Bikard, D., Jiang, W., Samai, P., Hochschild, A., Zhang, F., and Marraffini, L. A. (2013) Programmable repression and activation of bacterial gene expression using an engineered CRISPR-Cas system. *Nucleic Acids Res. 41*, 7429–7437.

(28) Kim, S. K., Han, G. H., Seong, W., Kim, H., Kim, S.-W., Lee, D.-H., and Lee, S.-G. (2016) CRISPR interference-guided balancing of a biosynthetic mevalonate pathway increases terpenoid production. *Metab. Eng. 38*, 228–240.

(29) Cleto, S., Jensen, J. V. K., Wendisch, V. F., and Lu, T. K. (2016) Corynebacterium glutamicum Metabolic Engineering with CRISPR Interference (CRISPRi). *ACS Synth. Biol. 5*, 375–385.

(30) Cress, B. F., Leitz, Q. D., Kim, D. C., Amore, T. D., Suzuki, J. Y., Linhardt, R. J., and Koffas, M. A. G. (2017) CRISPRi-mediated metabolic engineering of E. coli for O-methylated anthocyanin production. *Microb. Cell Fact. 16*, 10.

(31) Yao, L., Cengic, I., Anfelt, J., and Hudson, E. P. (2016) Multiple Gene Repression in Cyanobacteria Using CRISPRi. *ACS Synth. Biol. 5*, 207–212.

(32) Wu, M. Y., Sung, L. Y., Li, H., Huang, C. H., and Hu, Y. C. (2017) Combining CRISPR and CRISPRi Systems for Metabolic Engineering of E. coli and 1,4-BDO Biosynthesis. *ACS Synth. Biol. 6*, 2350–2361.

(33) Kim, S. K., Han, G. H., Seong, W., Kim, H., Kim, S. W., Lee, D. H., and Lee, S. G. (2016)

CRISPR interference-guided balancing of a biosynthetic mevalonate pathway increases terpenoid production. *Metab. Eng. 38*, 228–240.

(34) Lee, S. K., Chou, H., Ham, T. S., Lee, T. S., and Keasling, J. D. (2008) Metabolic engineering of microorganisms for biofuels production: from bugs to synthetic biology to fuels. *Curr. Opin. Biotechnol. 19*, 556–563.

(35) Gupta, P., and Phulara, S. C. (2015) Metabolic engineering for isoprenoid-based biofuel production. *J. Appl. Microbiol. 119*, 605–619.

(36) Kang, A., George, K. W., Wang, G., Baidoo, E., Keasling, J. D., and Lee, T. S. (2016) Isopentenyl diphosphate (IPP)-bypass mevalonate pathways for isopentenol production. *Metab. Eng. 34*, 25–35.

(37) Kang, A., Meadows, C. W., Canu, N., Keasling, J. D., and Lee, T. S. (2017) High-throughput enzyme screening platform for the IPP-bypass mevalonate pathway for isopentenol production. *Metab. Eng. 41*, 125–134.

(38) George, K. W., Thompson, M. G., Kang, A., Baidoo, E., Wang, G., Chan, L. J. G., Adams, P. D., Petzold, C. J., Keasling, J. D., and Soon Lee, T. (2015) Metabolic engineering for the high-yield production of isoprenoid-based C5 alcohols in E. coli. *Sci. Rep. 5*, 11128.

(39) Lee, T. S., Krupa, R. A., Zhang, F., Hajimorad, M., Holtz, W. J., Prasad, N., Lee, S. K., and Keasling, J. D. (2011) BglBrick vectors and datasheets: A synthetic biology platform for gene expression. *J. Biol. Eng. 5*, 15–17.

(40) Nielsen, A. A., and Voigt, C. A. (2014) Multi-input CRISPR/Cas genetic circuits that interface host regulatory networks. *Mol. Syst. Biol. 10*, 763–763.

(41) Cho, S., Choe, D., Lee, E., Kim, S. C., Palsson, B., and Cho, B. K. (2018) High-Level dCas9 Expression Induces Abnormal Cell Morphology in Escherichia coli. *ACS Synth. Biol. 7*,

1085–1094.

(42) Deltcheva, E., Chylinski, K., Sharma, C. M., Gonzales, K., Chao, Y., Pirzada, Z. A., Eckert, M. R., Vogel, J., and Charpentier, E. (2011) CRISPR RNA maturation by trans-encoded small RNA and host factor RNase III. *Nature 471*, 602–607.

(43) Yi, G., Sze, S. H., and Thon, M. R. (2007) Identifying clusters of functionally related genes in genomes. *Bioinformatics 23*, 1053–1060.

(44) Taboada, B., Ciria, R., Martinez-Guerrero, C. E., and Merino, E. (2012) ProOpDB: Prokaryotic operon database. *Nucleic Acids Res. 40*, 627–631.

(45) Price, M. N., Huang, K. H., Arkin, A. P., and Alm, E. J. (2005) Operon formation is driven by co-regulation and not by horizontal gene transfer. *Genome Res. 15*, 809–819.

(46) Garst, A. D., Bassalo, M. C., Pines, G., Lynch, S. A., Halweg-Edwards, A. L., Liu, R., Liang, L., Wang, Z., Zeitoun, R., Alexander, W. G., and Gill, R. T. (2016) Genome-wide mapping of mutations at single-nucleotide resolution for protein, metabolic and genome engineering. *Nat. Biotechnol. 35*, 1–14.

(47) Lo, C. A., Kays, I., Emran, F., Lin, T. J., Cvetkovska, V., and Chen, B. E. (2015) Quantification of Protein Levels in Single Living Cells. *Cell Rep. 13*, 2634–2644.

(48) Kramer, G., Sprenger, R. R., Nessen, M. A., Roseboom, W., Speijer, D., de Jong, L., de Mattos, M. J. T., Back, J., and de Koster, C. G. (2010) Proteome-wide Alterations in *Escherichia coli* Translation Rates upon Anaerobiosis. *Mol. Cell. Proteomics 9*, 2508–2516.

(49) Noh, M., Yoo, S. M., Kim, W. J., and Lee, S. Y. (2017) Gene Expression Knockdown by Modulating Synthetic Small RNA Expression in Escherichia coli. *Cell Syst. 5*, 418–426.e4.

(50) Nielsen, A. A., and Voigt, C. a. (2014) Multi-input CRISPR/Cas genetic circuits that interface host regulatory networks. *Mol. Syst. Biol. 10*, 763.

Table 1. Plasmids and strains. Strains with JBEI plasmid are available at JBEI public registry (https://public-registry.jbei.org) and searchable using JPUB number.

Plasmids	JPUB_number	Description	Reference
JBEI-18646	JPUB_011251	$P_{dCas9\text{-}Marraffini,}$ p15A, CmR	27
JBEI-18664	JPUB_011253	P_{Const}-dCas9-T1	This study
JBEI-18662	JPUB_011255	P_{Const}-dCas9-T2	This study
JBEI-18661	JPUB_011257	P_{Const}-dCas9-T3	This study
JBEI-18658	JPUB_011259	P_{Const}-dCas9-P1	This study
JBEI-18657	JPUB_011261	P_{Const}-dCas9-P2	This study
JBEI-18665	JPUB_011263	P_{Const}-dCas9-P3	This study
JBEI-18679	JPUB_011265	P_{Const}-dCas9-NT1	This study
JBEI-18676	JPUB_011267	P_{Const}-dCas9-NT2	This study
JBEI-18674	JPUB_011269	P_{Const}-dCas9-NT3	This study
JBEI-18647	JPUB_011271	P_{Tet}-wt-dCas9-NT1, p15A, CmR	This study
JBEI-18652	JPUB_011273	P_{Tet}-eng-dCas9-NT1, p15A, CmR	This study
JBEI-18653	JPUB_011275	P_{Tet}-wt-dCas9-P_{J23119}-NT1, p15A, CmR	This study
JBEI-18654	JPUB_011277	P_{Tet}-eng-dCas9-P_{J23119}-NT1, p15A, CmR	This study
JBEI-18655	JPUB_011279	P_{Tet}-wt-dCas9-P_{J23119}-NT1, pSC101, GmR	This study
JBEI-18648	JPUB_011281	P_{Tet}-eng-dCas9-P_{J23119}-NT1, pSC101, GmR	This study
JBEI-18670	JPUB_011283	P_{Tet}-wt-dCas9-nontarget, p15A, CmR	This study
JBEI-18669	JPUB_011285	P_{Tet}-eng-dCas9-nontarget, p15A, CmR	This study
JBEI-18667	JPUB_011287	JBEI-14034, P_{Tet}-wt-dCas9-P_{J23119}-nontarget, p15A, CmR	This study
JBEI-18692	JPUB_011289	JBEI-14034, P_{Tet}-eng-dCas9-P_{J23119}-nontarget, p15A, CmR	This study
JBEI-18689	JPUB_011291	JBEI-14034, P_{Tet}-wt-dCas9-P_{J23119}-nontarget, pSC101, GmR	This study
JBEI-18697	JPUB_011293	JBEI-14034, P_{Tet}-eng-dCas9-P_{J23119}-nontarget, pSC101, GmR	This study
JBEI-18706	JPUB_011369	JBEI-14034, P_{Tet}-wt-dCas9-P_{J23119}-nontarget, pSC101, KanR	This study
JBEI-18707	JPUB_011371	JBEI-14034, P_{Tet}-eng-dCas9-P_{J23119}-nontarget, pSC101, KanR	This study
JBEI-18698	JPUB_011367	P_{J23100}-RFP-GFP, p15A, KanR	This study
JBEI-18650	JPUB_011295	P_{Tet}-wt-dCas9-P_{J23119}-P1, pSC101, GmR	This study
JBEI-18651	JPUB_011297	P_{Tet}-wt-dCas9-P_{J23119}-RFPNT, pSC101, GmR	This study
JBEI-18649	JPUB_011299	P_{Tet}-wt-dCas9-P_{J23119}-GFPNT, pSC101, GmR	This study
JBEI-18671	JPUB_011301	P_{Tet}-eng-dCas9-P_{J23119}--P1, pSC101, GmR	This study
JBEI-18672	JPUB_011303	P_{Tet}-eng-dCas9-P_{J23119}-RFPNT, pSC101, GmR	This study
JBEI-18673	JPUB_011305	P_{Tet}-eng-dCas9-P_{J23119}-GFPNT, pSC101, GmR	This study
JBEI-18684	JPUB_011307	DH1, P_{Tet}-wt-dCas9-P_{J23119}-poxB, pSC101, KanR	This study
JBEI-18681	JPUB_011309	DH1, P_{Tet}-wt-dCas9-P_{J23119}-ackA, pSC101, KanR	This study
JBEI-18663	JPUB_011311	DH1, P_{Tet}-wt-dCas9-P_{J23119}-pta, pSC101, KanR	This study
JBEI-18686	JPUB_011313	DH1, P_{Tet}-wt-dCas9-P_{J23119}-poxB-ackA-pta, pSC101, KanR	This study
JBEI-18704	JPUB_011315	DH1, P_{Tet}-eng-dCas9-P_{J23119}-poxB, pSC101, KanR	This study
JBEI-18705	JPUB_011317	DH1, P_{Tet}-eng-dCas9-P_{J23119}-ackA, pSC101, KanR	This study

JBEI-18702	JPUB_011319	DH1, P_{Tet}-eng-dCas9-P_{J23119}-pta, pSC101, KanR	This study
JBEI-18703	JPUB_011321	DH1, P_{Tet}-eng-dCas9-P_{J23119}-poxB-ackA-pta, pSC101, KanR	This study
JBEI-3279	JPUB_000262	pBbS0k	37
JBEI-18687	JPUB_011323	P_{Tet}-wt-dCas9-P_{J23119}-arcC, pSC101, KanR	This study
JBEI-18660	JPUB_011325	P_{Tet}-wt-dCas9-P_{J23119}-yahI, pSC101, KanR	This study
JBEI-18700	JPUB_011327	P_{Tet}-wt-dCas9-P_{J23119}-yqeA, pSC101, KanR	This study
JBEI-18690	JPUB_011329	P_{Tet}-wt-dCas9-P_{J23119}-gltA, pSC101, KanR	This study
JBEI-18683	JPUB_011331	P_{Tet}-wt-dCas9-P_{J23119}-accA, pSC101, KanR	This study
JBEI-18668	JPUB_011333	P_{Tet}-wt-dCas9-P_{J23119}-eutD, pSC101, KanR	This study
JBEI-18675	JPUB_011335	P_{Tet}-wt-dCas9-P_{J23119}-deoB, pSC101, KanR	This study
JBEI-18678	JPUB_011337	P_{Tet}-wt-dCas9-P_{J23119}-ppc, pSC101, KanR	This study
JBEI-18701	JPUB_011339	P_{Tet}-wt-dCas9-P_{J23119}-yhfW, pSC101, KanR	This study
JBEI-18659	JPUB_011341	P_{Tet}-wt-dCas9-P_{J23119}-thrC, pSC101, KanR	This study
JBEI-18693	JPUB_011343	P_{Tet}-wt-dCas9-P_{J23119}-ispA, pSC101, KanR	This study
JBEI-18680	JPUB_011345	P_{Tet}-wt-dCas9-P_{J23119}-mdh, pSC101, KanR	This study
JBEI-18685	JPUB_011347	P_{Tet}-wt-dCas9-P_{J23119}-asnA, pSC101, KanR	This study
JBEI-18677	JPUB_011349	P_{Tet}-wt-dCas9-P_{J23119}-prpE, pSC101, KanR	This study
JBEI-18666	JPUB_011351	P_{Tet}-wt-dCas9-P_{J23119}-gldA, pSC101, KanR	This study
JBEI-18682	JPUB_011353	P_{Tet}-wt-dCas9-P_{J23119}-mqo, pSC101, KanR	This study
JBEI-18695	JPUB_011355	P_{Tet}-wt-dCas9-P_{J23119}-maeB, pSC101, KanR	This study
JBEI-18694	JPUB_011357	P_{Tet}-wt-dCas9-P_{J23119}-dacA, pSC101, KanR	This study
JBEI-18691	JPUB_011359	P_{Tet}-wt-dCas9-P_{J23119}-asnA-gldA, pSC101, KanR	This study
JBEI-18696	JPUB_011361	P_{Tet}-wt-dCas9-P_{J23119}-asnA-prpE, pSC101, KanR	This study
JBEI-18656	JPUB_011363	P_{Tet}-wt-dCas9-P_{J23119}-gldA-prpE, pSC101, KanR	This study
JBEI-18688	JPUB_011365	P_{Tet}-wt-dCas9-P_{J23119}-asnA-gldA-prpE, pSC101, KanR	This study

Strains	**Description**	**Reference**
JBEI-14034 (JPUB_011194)	MG1655 trxA::P3-BCD2-RFP-FRT-Km	This study
C0-nontarget	JBEI-14034 + JBEI-18646	This study
T1	JBEI-14034 + JBEI-18664	This study
T2	JBEI-14034 + JBEI-18662	This study
T3	JBEI-14034 + JBEI-18661	This study
P1	JBEI-14034 + JBEI-18658	This study
P2	JBEI-14034 + JBEI-18657	This study
P3	JBEI-14034 + JBEI-18665	This study
NT1	JBEI-14034 + JBEI-18679	This study
NT2	JBEI-14034 + JBEI-18676	This study
NT3	JBEI-14034 + JBEI-18674	This study
C1	JBEI-14034 + JBEI-18647	This study
C2	JBEI-14034 + JBEI-18652	This study
C3	JBEI-14034 + JBEI-18653	This study
C4	JBEI-14034 + JBEI-18654	This study
C5	JBEI-14034 + JBEI-18655	This study
C6	JBEI-14034 + JBEI-18648	This study

C1-nontarget	JBEI-14034 + JBEI-18670	This study
C2-nontarget	JBEI-14034 + JBEI-18669	This study
C3-nontarget	JBEI-14034 + JBEI-18667	This study
C4-nontarget	JBEI-14034 + JBEI-18692	This study
C5-nontarget	JBEI-14034 + JBEI-18689	This study
C6-nontarget	JBEI-14034 + JBEI-18697	This study
C7-nontarget	JBEI-14034 + JBEI-18706	This study
C8-nontarget	JBEI-14034 + JBEI-18707	This study
C5P	JBEI-18698 + JBEI-18650	This study
C5RFPNT	JBEI-18698 + JBEI-18651	This study
C5GFPNT	JBEI-18698 + JBEI-18649	This study
C6P	JBEI-18698 + JBEI-18671	This study
C6RFPNT	JBEI-18698 + JBEI-18672	This study
C6GFPNT	JBEI-18698 + JBEI-18673	This study
C5-poxB	DH1, JBEI-18684	This study
C5-ackA	DH1, JBEI-18681	This study
C5-pta	DH1, JBEI-18663	This study
C5-poxB-ackA-pta	DH1, JBEI-18686	This study
C6-poxB	DH1, JBEI-18704	This study
C6-ackA	DH1, JBEI-18705	This study
C6-pta	DH1, JBEI-18702	This study
C6-poxB-ackA-pta	DH1, JBEI-18703	This study
DH1-empty	DH1, JBEI-3279	This study
ΔpoxBΔackAΔpta	JBEI-3606	This study
DH1-knockout	JBEI-3606 + JBEI-3279	This study
$KG1_{R10}$	JBEI-15391	36
Base strain	JBEI-15391 + JBEI-3279	This study
C5-arcC	JBEI-15391 + JBEI-18687	This study
C5-yahI	JBEI-15391 + JBEI-18660	This study
C5-yqeA	JBEI-15391 + JBEI-18700	This study
C5-gltA	JBEI-15391 + JBEI-18690	This study
C5-accA	JBEI-15391 + JBEI-18683	This study
C5-eutD	JBEI-15391 + JBEI-18668	This study
C5-deoB	JBEI-15391 + JBEI-18675	This study
C5-ppc	JBEI-15391 + JBEI-18678	This study
C5-yhfW	JBEI-15391 + JBEI-18701	This study
C5-thrC	JBEI-15391 + JBEI-18659	This study
C5-ispA	JBEI-15391 + JBEI-18693	This study
C5-mdh	JBEI-15391 + JBEI-18680	This study
C5-asnA	JBEI-15391 + JBEI-18685	This study
C5-prpE	JBEI-15391 + JBEI-18677	This study
C5-gldA	JBEI-15391 + JBEI-18666	This study
C5-mqo	JBEI-15391 + JBEI-18682	This study

C5-maeB	JBEI-15391 + JBEI-18695	This study
C5-dacA	JBEI-15391 + JBEI-18694	This study
C5-asnA-gldA	JBEI-15391 + JBEI-18691	This study
C5-asnA-prpE	JBEI-15391 + JBEI-18696	This study
C5-gldA-prpE	JBEI-15391 + JBEI-18656	This study
C5-asnA-gldA-prpE	JBEI-15391 + JBEI-18688	This study